韓國海洋工學會誌 第12卷 第3號, pp.42~48, 1998. 8

◉ 論 文

Cracking of S2 Ice by Spherical Indentation

Sang-Ryong Ko*

(98년 3월 23일 접수)

구형관입에 의한 S2 얼음의 균열

고 상 용*

Key Words : Monotonic load(단조증가하중), Pulsed load(맥박하중), Cracking behavior(균열거동), Half penny cracks(반동전균열), Radial cracks(방사선균열), Lateral cracks(횡균열)

Abstract

구형 관입시험에 의한 얼음의 균열을 연구 하였다. -10℃에서 S2 기둥얼음의 시편(152mm X 152mm X 152mm)에 stainless 강으로 된 구(지름 25.4mm)로 하중을 가하였다. 구형 indentor 는 얼음 시편의 장축인 기둥방향에 수직으로 하중을 가하였으며 이때 변위율은 0.038mm/s로 하여 단조증가 하중 시험을 하였다. 하중을 가하기 시작하면 indentor 하부에서 crushing 이 발생하고, 하중이 증가 함에 따라서 방사선 균열 또는 횡균열이 성장하여 splitting 또는 spallation 이 발생 하였다. 단조증가 하중 때와 동일한 indentor를 사용하여 하중 및 비하중율 0.5 KN/s로 맥박하중을 가할 때 이들 방사선 균열 및 횡 균열이 발생 성장 하였다.첫 맥박 하중의 크기는 1KN으로 하고 그 뒤 계속 이어지는 시험은 맥박 하중 의 크기를 증가시킨 뒤 행하였으며 균열 길이는 맥박과 맥박 사이에서 계측 하였다. 기타 취성고체에서 관찰 되었던 것과 같이 방사선 균열 및 측면균열의 길이는 impression 반지름과 하나의 지수법칙이 성립함을 보여주었다.

1. Introduction

Ice indentation has been extensively studied by a number of authors. Of those studies, the ones that are most applicable to study at hand are Timco et al [1], Gagnon [2], Jordaan et al [3] and Grape & Schulson [4] report valuable results on the crushing of ice, the crushing and clearance of ice by spherical indentor and the confinement problems by square indentor. Many papers published especially for indentation brittleness by spherical indentor in glasses and ceramics. Pure elastic deformation and the geometry of the contact zone for a sample surface has been predicted by Hertz [5]. This stress field was first analyzed by Huber [6]. The processes of Hertzian indentation fracture of brittle solids are reasonably well understood

* 정회원, 울산대학교 수송시스템공학부

by Lawn and Wilshaw[7]. The analysis for the nature of elastic/plastic indentations is explained comparatively in detail by Lawn and Fuller [8] and Swain and Hagan [9]. Indentation crack length measurements are now almost universal for fracture property assessments of ceramics. In this paper deals with only the typical columnar fresh-water ice on the rivers, lakes and ponds (Fig. 1). This ice is called S2 fresh-water ice and the crystallographic c-axes are more or less confined to the horizontal plane, randomly oriented within this plane (Michel et al, [10]). Blunt indentor-static load contact from four types of indentation fracture approaches classified by Wiederhorn et al [11] and one domain, indentation method of two domains defined by Timco are used to study the crack phenomena of S2 ice. The pure elastic deformation and the geometry of the contact zone for spherical indentation by Hertz and the cracks theory and geometry by Lawn et al are applied to investigate the followings: relation between the load and the impression size, size of normal pressures for the center of loaded circle and geometric phenomena of the cracks during the indentation tests.

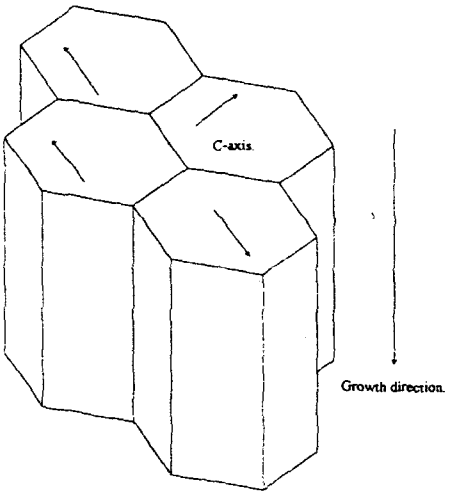

Fig. 1 S2 Columnar fresh water ice

2. Experimental Procedure

2.1. Sample

The samples used are made from S2 columnar fresh-water ice and the size of those samples is 152mm cube. The average grain diameter of the ice sample is 6 ± 1 mm and the crystallographic c-axis are more or less confined to the horizontal plane, randomly oriented within this plane.

2.2. Indentor

The indentor used is made of #52100 alloy steel sphere with its radius, 12.7mm, Youngs modulus, E=205GPa and Poisson ratio, $\nu = 0.295$.

2.3. Apparatus and procedure

Indentation experiments are to be carried out at a displacement rate of $\dot{\delta} = 3.8 \times 10^{-2}$ for monotonic loading and at a loading and

Fig. 2 Front view of Uniaxial Testing Machnine.

unloading rate of 0.5KN/sec for pulsed loading at -10℃ temperature with the Uniaxial Testing Machine at Thayer School Ice Research Laboratory, Fig. 2.

3. Results

Twenty-one tests in total, five tests for monotonic and sixteen tests for pulsed loading were carried out to get the following results.

3.1 Load versus displacement

Fig. 3(a) and 3(b) are indicated by load displacement curves in monotonic load tests. Those curves are so similar to each others in shape. The yielding points are scattered from 3.00KN to 5.20KN. The spallations occur at around 7.5KN load as Fig. 3(a). Fig. 4(a) and 4(b) show the load-displacement curves in pulsed load tests. The splitting occurs at around

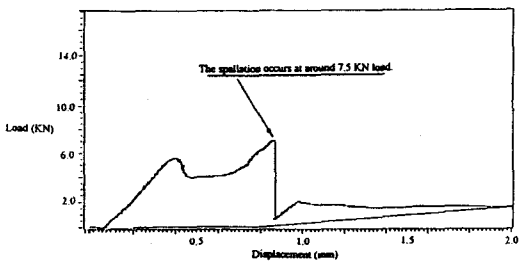

(a)

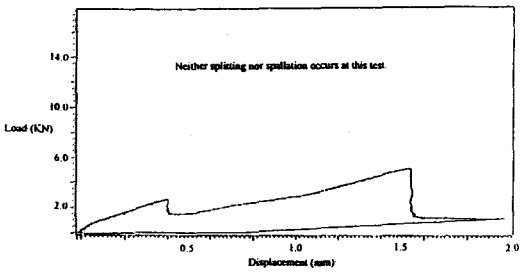

(b)

Fig. 3 Load-displacement curve by monotonic lo ad.

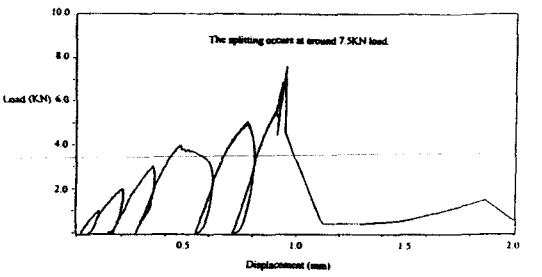

(a)

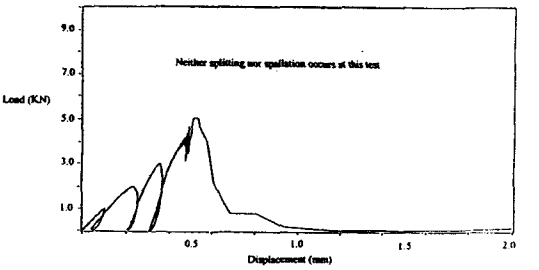

(b)

Fig. 4 Load-displacement curve by pulsed load (The load increase by 1KN)

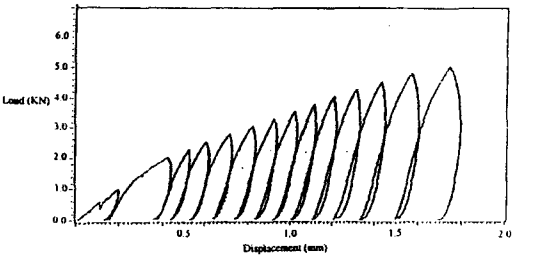

(a)

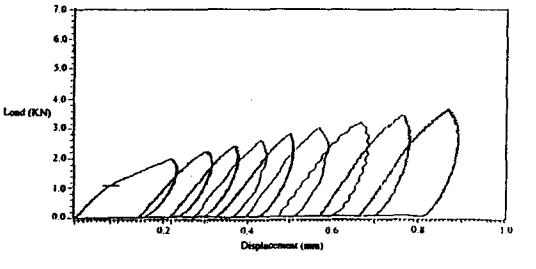

(b)

Fig. 5 Load-displacement curve by pulsed load

7.5KN of load as Fig. 4(a). As shown those curves had the hysteresis loops. Author recognized from several tests results that the splitting or the spallation had occurred at around 7.5KN of load. This load was called as a critical load, Pc. Hereafter all tests were carried out under Pc, for example Fig. 5(a) and 5(b), at loads of 1KN, 2.0KN, 2.25KN, 2.5KN, ..., 4.75KN, 5KN, and 1KN, 2.0KN, 2.20KN, 2.40KN, ...,3.8KN, respectively.

3.2 Crack Patterns

Fig. 6 represents schematically the most relevant fracture geometries, corresponding with the observation of the cracking behavior, which are listed below the radial cracks initiated under and around the impression. We use the notations of directions, X1, X2, and X3 as in the papers of Schulson [12]. X1 is the load direction and X3 is the columnar direction. At load of 1KN, the pulverized zone, the surface radial cracks and subsurface radial cracks were shown on the sample. At load of 3KN, the median crack initiated from the pulverized zone. At load of 4.25KN, the two saucer-like lateral cracks initiated from the pulverized zone under the

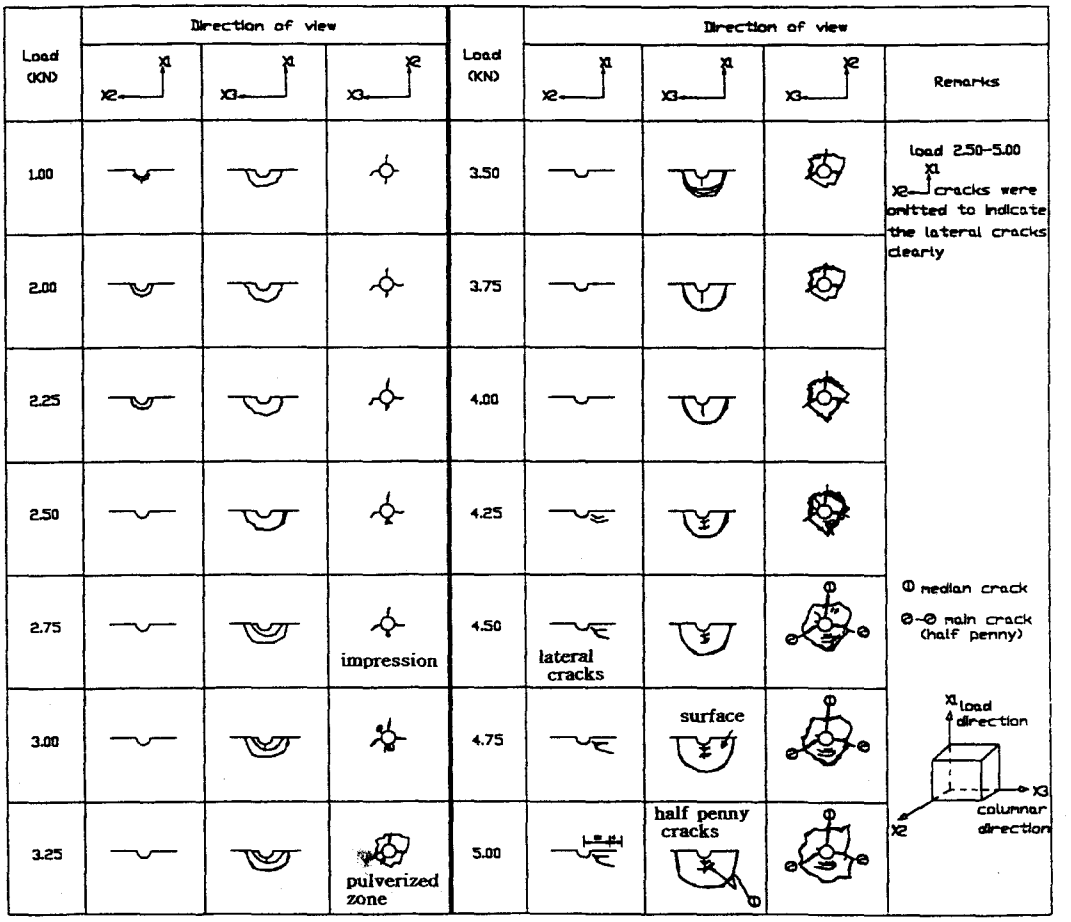

Fig. 6 A schematic drawing of a pulsed loading test results. It shows the crack extensions according to increase loading and coordinate system in Remarks.

indentor. The main cracks appeared on both sides of the pulverized zone. Some cracks were omitted at X1 - X2 views to see the two saucer-like lateral cracks clearly. Several test results were similar to the case of Fig. 6.

3.3 Crack Length versus Impression Radius

Fig. 7 shows the plots of the crack lengths obtained from the tests results.

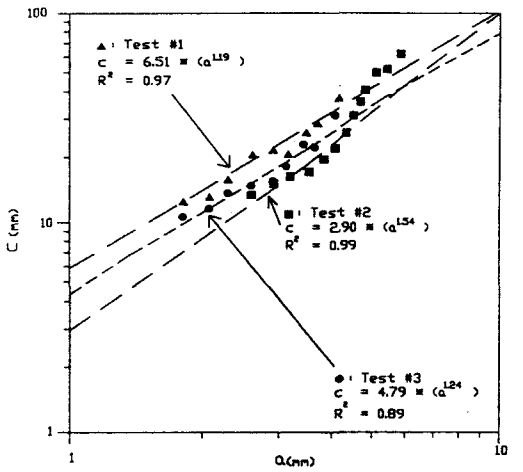

Fig. 7 Crack length as a function of impression radius.

4. Discussion

The theories of crack initiation are not discussed in this paper but are comprehensively reviewed by Lawn and Wilshaw.

4.1. Formulation

In Hertzian elastic contact, the impression radius a is given by

$$a = (3PR/4E^*)^{(1/3)} \quad (1)$$

Where P is the applied load, R is the radius of indentor and E^* is given by

$$1/E^* = (1-\nu_1^2)/E_1 + (1-\nu_2^2)/E_2$$

Youngs modulus of E_1, E_2 and Poissons ratio ν_1, ν_2 of the sample and sphere respectively. Displacement, is given by

$$\delta = a^2/R \quad (2)$$

Normal pressure P_0 is given by for the center of the loaded circle

$$P_0 = 3P/2\pi a^2 \quad (3)$$

Lawn et al derived the relationship for crack length, c, and impression radius, a as follows

$$(K_{IC}/H a^{1/2})(H/E)^{1/2} \propto (c/a)^{-3/2} \quad (4)$$

Where K_{IC} is the fracture toughness, H is the hardness of S2 ice. This expression has become the norm in the ceramics indentation fracture literature. Put $P_0 = H$, Equation (4) is changed as follow,

$$(P_o E/K_{IC}^2) \propto c^3/a^4 \quad (5)$$

If put it into a constant of brittle parameter, B, Equation (5) reduce to.

$$c \propto Ba^{4/3} \quad (6)$$

Equation (6) changed as following

$$c = f(a) \quad (7)$$

Where f is a function of brittleness.

4.2 Comparison of the results

Table 1 shows the values of the normal pressure for the center of loaded circle, P_0 and impression radius, a obtained by the test rusults. The melting pressure from ice into water is 100MPa in the phase diagram as shown Fig. 8 [13]. According to the test results, the values of normal pressure for the center of the loaded circle, P_0 at the peak loads are from 127MPa to 429MPa. There may be water particles under the indentor. For the fully elastic

indentation, the value of a is around 2.5mm at the load of 9KN. As increased the load more than 9KN, the value of a is not increased so much. However according to the results of test, the measured value of a increased to 5.5mm. Fig. 7 shows that the exponent average value of 1.33 for measured radial cracks is in close agreement with Lawn and coworkers' Equation(5). Equation(6) and (7) are the reduced forms of Equation(5). These Equations indicate the relation between the crack length and the impression radius clearly. The value of B is not considered in this paper

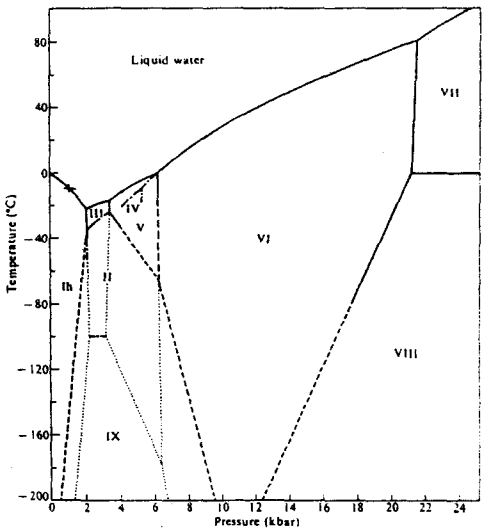

Fig. 8 Phase diagram of the solid phases of water

+ Symbol is the cross point of horizontal line of -10℃ abscissa and perpendicular line of 100MPa ordinate.

Table 1 Monotonic load tests results

Test peak	Test 1		Test 2	
	1st Peak	1nd Peak	1st Peak	2nd Peak
P(KN)	5.5	7.05	2.65	5.2
a(mm)	2.31	3.32	2.31	4.42
P_0(Mpa)	492	305	237	127
δ (mm)	0.42	0.87	0.42	1.54

4.3 Crack phenomena

There are two important crack systems originate in the pulverized zone of the ice sample produced by the sphere indentation at large contact loads (1KN and over). These are the radial/median crack system and lateral crack system. Radial/median cracks are formed perpendicular to the sample surface. Saucer-like lateral cracks form closely parallel to the sample surface. The first cracks to form during loading of an indentation are the shallow radial cracks (the Palmqvist cracks). As the load increased the cracks progressed to greater depths so that they approximated half-penny like cracks and median cracks surrounding the pulverized zone. Lateral cracking is mostly apparent at large contact loads, above 4.00KN load. When the pulsed loading were increased by 0.25KN or 0.20KN, two main radial cracks occurred at the center of the impression(② - ② in Fig. 6) made of the angle (from 110° -180°).

Both sides of two main radial cracks, half penny like cracks have the saucer-like lateral cracks at small side of the angle and the median cracks at large side.

5. Conclusions

The main results obtained in this study are the following

1. The splitting or the spalling occurs on the samples less than 7.5 KN of load in the spherical indentation tests. There was no sign of Hertzian ring cracks and cone cracks on the samples by the spherical indentation.

2. P_0 normal pressures for the center of loaded circle at the peak loads are higher than the melting pressure at the temperature -10℃. There may be water particles under the indentor.

3. In pulsed loading, the radial cracks, the

half-penny cracks are initiated just like a glasses and ceramics by the sharp or blunt indentor-static or impact loading. Both sides of the half-penny like cracks have the saucer-like lateral cracks at one side and the other side radial cracks.

4. These test-results are substantially similar to the values of glasses and ceramic cases. There must be the constant correlations between the crack sizes and the sizes of impressions.

The parameters of the crack patterns and the crack sizes of S2 ice are expected to study more in detail by someone interested in.

References

1. G. W. Timco, Indentation and Penetration of Edge-Loaded Freshwater Ice Sheets in the Brittle Range Proc. OMAE 4 pp.444-452 1986.
2. R. E. Gagnon, Generation of Melt during Crushing Experiments on Fresh-water Ice CRS and T 2 pp.385-398 1994.
3. Ian J. Jordaan et al, The Crushing and Clearing of Ice in Fast Spherical Indentation Tests Proc. the Seventh Int. Confer. Offshore Mecha. and Arcti Eng. 4 pp.111-116 1988.
4. J.A, Grape and E. M. Schulson , The Effect of Confinement on the Brittle Indentatiion Failue of Ice. The 15th Annual Advisory Board Meeting of the Ice Research Program pp.50-59 1997.
5. H. Hertz, On the Contact of Elastic Solids (in Ger.) Zeirschrift fur die Reine und Angewandte Mathematic, 92 pp.146-162 1981.
6. M. T. Huber, On the Theory of Contacting Solid Elastic Bodies (in Ger.), Ann. Phys. 14 pp.153-163 1904.
7. B. R. Lawn and T. R. Wilshaw, Indentation Fracture: Principles and Applications, J. Mater. Sci.10, pp.1049-1081 1975.
8. B. R. Lawn and E. R. Fuller, Equilibrium Penny-Like Cracks in Indentation Fracture. J. Mater. Sci, 10 , pp.2016-2020 1975.
9. M. V. Swain anf J. T. Hagan, Indentation Plasticity and the Ensuing Fracture of Glass, J. Phys. D: Appl. Phys. 9 . pp.2201-2214 1976.
10. B. Michel and R. O. Ramseier, Classification of River and Lake Ice J. Can. Geo. 8 36 pp.36-41 1971.
11. S. M. Wiederhorm et al, Strength Degradation of Glass Impacted with Sharp Particles; I, Anealed Surfaces. J. Amer. Cera. Soci. 62 pp.66-70 1979.
12. E. M. Schulson, The Failure of Ice under Compression The Mineral, Metals & Materials Society. The Johannes Weertman Symposium pp.363-374 1996.
13. P. V. Hobbs, Ice Physics Clarendon Press, Oxford, 1974.